Criticality Analysis of Biblis 2D Reactor via Diffusion Theory

Nicholas March

Dr. Wei Ji
Radiation Transport Methods
19 December 2023

Table of Contents

Abstract

Criticality, leakage rate distributions, and flux distributions for a two-group 2D eigenvalue problem pertaining to the Biblis 2D reactor geometry were computed using diffusion theory, yielding a k_{eff} value of 1.168066 after 450 iterations with a discretized cell size of 5.78065 cm, a 13.95% difference from the expected k_{eff} value of 1.025105.

Background

The reactor schematic shown in Figure 1 represents a simplified radial slice or cross-section of the Biblis Nuclear Power Plant, which was a pressurized water reactor that operated from 1974 to 2011 in Germany. Simulating a 2D representation of a 3D reactor avoids the computational and mathematical complexity of 3D finite volume methods while still capturing key neutron behavior and criticality information. Similarly, by selecting a two-group neutron energy scheme, a distinction is made between high-energy neutrons produced in fission events and lower-energy neutrons responsible for sustaining the chain reaction. Inclusion of more energy groups yields diminishing returns in the context of this analysis and further complicates the algorithms involved, hence the implementation of a two-group energy approximation.

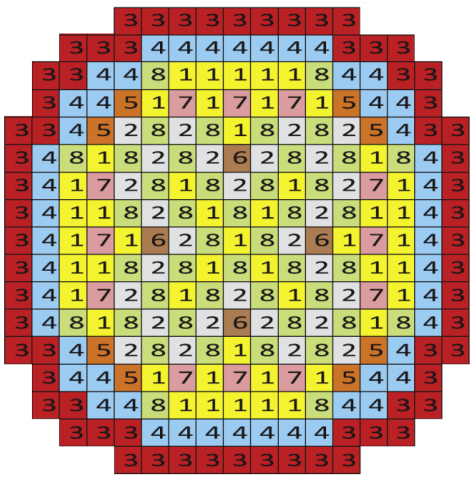

Figure 1: Biblis 2D Reactor Schematic

Several key assumptions were made to streamline the computational process. Isotropic scattering is assumed, simplifying the angular dependency calculations of neutron flux. Upscattering is neglected, based on the rationale that in a thermal reactor setting, lower energy neutrons gaining energy upon scattering is a rare event, thus $\Sigma_{1\leftarrow 2}$ is set to zero. For the outer perimeter of the reactor core, vacuum boundary conditions are applied, representing an absence of incoming neutron flux from outside. The spaces in the corners of the diagram given in Figure 1 were filled in as vacuum or void, denoted as material 0, to simplify the computational approach. This vacuum material was assigned values of zero for all material properties. The prior assumption is partly incorrect, as it includes assigning the vacuum diffusion coefficient as zero which implies neutrons stream freely. During some testing, this resulted in neutron flux in the vacuum areas equivalent to infinity, which actually provides a very useful indicator of where

the void begins. This process does not follow physical theory but is meant to work around computational issues; setting diffusion coefficients equal to infinity would raise many errors. To remedy this, infinite fluxes in the void areas were set to the actual expected value of zero. The outer boundary's length for leakage is determined by the extrapolation length, set as 0.7104 λ_{tr}, aligning with standard practices in reactor physics for modeling neutron leakage and ensuring an accurate representation of leakage rates. These assumptions, while reducing complexity, are in line with typical modeling practices in reactor physics and are essential for a focused yet robust analysis of the reactor core's neutron behavior.

Discretization Scheme

To derive cell-edge 2D discretization of the diffusion equation, first start with the 2D diffusion equation, given below as Equation 1. For a two-group analysis, Equation 1 is a system of two equations, one for each energy. The main difference lies in the material properties, as well as the source term S(x,y) which will be discussed in more detail later on.

$$\frac{\partial}{\partial x}D(x,y)\frac{\partial}{\partial x}\phi(x,y) + \frac{\partial}{\partial y}D(x,y)\frac{\partial}{\partial y}\phi(x,y) + \Sigma_a(x,y)\phi(x,y) = S(x,y) \quad \text{(Eq. 1)}$$

First impose a grid or mesh on the geometry of the system, in this case with the points at the cell edges. The result of this is that there are J+1 points for J cells. The unknown values are placed at the edge intersections of cells as opposed to at their centers, making calculation of leakage much simpler. The conservation equation is then integrated over the area A_{ij}, which represents the area of one cell in the discretization scheme. Due to the selection of cell-edge discretization, interactions at a particular (x, y) position are influenced by the materials of the four quadrants or cells surrounding it. This necessitates the taking of an average for relevant material properties like cross sections and the diffusion coefficient. One vital requirement is that the cell size yields a mesh that fits entirely and perfectly within the geometry of the core. As a result, discretization cell width h is chosen to be proportional to the reactor unit side length R_{sl}. Specifically, this analysis investigated h = R_{sl}, h = 0.5 R_{sl}, and h = 0.25 R_{sl}. Selecting non-proportional values of h throws errors during plotting and significantly increases time to convergence, if the solution converges at all. The height of the discretization cell was chosen to be equivalent to the width, meaning that $A_{ij} = h^2$. This greatly reduces the complexity of the resulting discretized equations and accompanying code. The problem can be further simplified with the introduction of the global number index given in Equation 2, which allows for the (i, j) indexes of an J x J matrix to be converted to a single index n pertaining to 1D array with length J * J. The form of this equation is particularly for number systems starting at zero, like in Python. This is similar to using the flatten() command from Numpy, which turns a 2D matrix into a 1D array.

$$n = (j * J) + i \quad \text{(Eq. 2)}$$

Applying the previously mentioned simplifications and integration steps to the 2D diffusion equation yields the following discretized equation, given as Equations 3.1 through 3.6.

$$a_{n,n-J}\phi_{n-J} + a_{n,n-1}\phi_{n-1} + a_{n,n}\phi_{n} + a_{n,n+1}\phi_{n+1} + a_{n,n+J}\phi_{n+J} = S_n A_n \quad \text{(Eq. 3.1)}$$

$$a_{n,n-I} = -\frac{D_{i-1,j-1}+D_{i,j-1}}{2} \quad \text{(Eq. 3.2)}$$

$$a_{n,n-1} = -\frac{D_{i-1,j-1}+D_{i-1,j}}{2} \quad \text{(Eq. 3.3)}$$

$$a_{n,n} = \frac{D_{i-1,j-1}+D_{i,j-1}}{2} + \frac{D_{i-1,j-1}+D_{i-1,j}}{2} + \frac{D_{i,j-1}+D_{i,j}}{2} + \frac{D_{i-1,j}+D_{i,j}}{2} + \bar{\Sigma}_{rij}A_{ij} \quad \text{(Eq. 3.4)}$$

$$a_{n,n+1} = -\frac{D_{i,j-1}+D_{i,j}}{2} \quad \text{(Eq. 3.5)}$$

$$a_{n,n+1} = -\frac{D_{i-1,j}+D_{i,j}}{2} \quad \text{(Eq. 3.6)}$$

In Equation 3.4, $\bar{\Sigma}_{rij}$ represents the macroscopic removal cross section averaged across the four cells around a particular grid point. In equation 3.1, S_n is the source term. For energy group one, the source term consists of just the fission source, which is equivalent to the product of the neutron flux of the past generation, nu, and the macroscopic fission cross section. In addition to the fission source, energy group two's source term also includes a downscattering term, which represents neutrons scattering from group one into group two. It is equivalent to the product of the neutron flux of group one in this generation and the downscattering macroscopic cross section. The importance of this is that the conservation equations for group one and group two are coupled. To solve for group 2, the flux of group 1 must first be found. As previously mentioned, a zero flux or vacuum boundary condition was imposed on the boundaries of the active core geometry. This is represented mathematically by setting neutron flux equal to zero at the boundaries or edges, as shown in Equation 4. The assumption of zero flux at the boundary allows for the calculation of neutron leakage via the extrapolation length, flux just inside the boundary, and diffusion coefficients. Special attention must be paid to corner cells, which have leakage through both a horizontal and a vertical face.

$$\phi_{edge} = 0 \quad \text{(Eq. 4)}$$

Equation 3.1 can be rewritten by defining a diffusion matrix M_d and a fission source matrix M_f, as shown below in Equation 5. This equation can be solved with Gauss-Seidel iterative method, and yields an unnormalized flux which must be corrected with the criticality value of the current and last generations, as shown in Equation 7. As mentioned before, the two-group approximation means two sets of fluxes and by extension two sets of matrices must be found. In addition, calculating the criticality requires the combination of the flux from groups one and two, which is shown in Equation 6.

$$M_d \phi^{(l+1/2)} = \frac{1}{k^l} M_f \ \phi^l \quad \text{(Eq. 5)}$$

$$k^{(l+1)} = \frac{1}{k^l}\left(M_{f,g1}\phi_{g1}^{(l+1/2)} + M_{f,g2}\phi_{g2}^{(l+1/2)}\right) \qquad \text{(Eq. 6)}$$

$$\phi_g^{l+1} = \frac{k^{l+1}}{k^l}\phi_g^{(l+1/2)} \qquad \text{(Eq. 7)}$$

Solution Strategy

One of the most difficult challenges associated with this geometry is determining what materials to use where. To address this, the first step of the computational solution involved constructing a geometry matrix which contains the material numbers in a 17 x 17 grid representing the reactor core sections, as well as a function used to determine material at a given (x, y) location in the actual geometry. This function returns the material number, which can then be used to index matrices which contain relevant properties for each material and energy group. As previously stated, the mesh sizes tested were proportional to the length of the reactor core sections, specifically h = R_{sl}, h = 0.5 R_{sl}, and h = 0.25 R_{sl}. The next step involves defining the diffusion and fission coefficient matrices, which come from the equations given in the previous section and are both of shape (J+1) x (J+1). Particular care must be taken around the boundaries of the active core geometry, due to the fact that certain terms must be left off in the coefficient matrices for those areas. To preserve the results of the linear algebra, cells with vacuum material are inputted in the diffusion coefficient matrix as just ones in the diagonal. Setting them to zero in the source matrix yields a flux of zero in the vacuum, which agrees with the prescribed boundary conditions. The inverse of the sum of the diagonal of the respective fission coefficient matrix is used as the initial guess for the flux for each group, and 1.0 is used as the initial guess for criticality. Using the Gauss-Seidel iterative method with convergence tolerance 1 x 10^{-6}, the flux for group one can be solved from Equation 5 using its coefficient matrices and the initial guesses. Now that the group one neutron flux is known, it can be used to construct the source coefficient matrix for group two, which allows for group two neutron flux to be solved similarly using its initial flux guess and diffusion coefficient matrix. With these two sets of flux values for the first generation, a new criticality can be calculated. This value, along with the two flux values, are passed into the next iteration of the loop and used as the new guesses. Convergence occurs when the difference between subsequent criticality values drops below 1 x 10^{-6} and the difference between subsequent flux values for both groups drops below 1 x 10^{-5}. Following convergence, the effective criticality, or maximum of the previously calculated criticality values, is outputted along with the number of iterations required. Final flux distributions for groups one and two are used to calculate leakage as previously described, using boolean logic to differentiate corners and vertical or horizontal faces. Leakage and flux distributions are plotted for ease of viewing. A number of minor functions were implemented but do not warrant explanation, see appendix for full code and function descriptions.

Results and Observations

Plots depicting the diffusion matrix M_d and the source matrix M_f are shown below in Figures 2 and 3, respectively. These plots were produced using the matrices from the h = R_{sl} case, due to the fact that it exemplifies the expected structure the best. This is due to the fact that as the size of the matrices gets very large, such as for h = 0.25 R_{sl}, the sparsity of the matrix also gets very large, meaning most of the useful behavior is obscured by all of the zeros. This results in plots of the diffusion matrix appearing to be a single diagonal, even though it is actually five diagonals that are spaced very close together. The examination of the matrix visualization plots reveals a clear delineation between active reactor materials and void regions. The off-diagonal elements in the diffusion coefficient matrix suggest interactions between neighboring cells within the geometry, with further off-diagonals corresponding to cells in adjacent rows and closer off-diagonals to left and right neighbors. The primary diagonal is representative of the cell in question, underscoring the localized nature of the diffusion process within each cell. The source coefficient matrix, on the other hand, only contains non-zero values on the main diagonal, due to the fact that the source term is only a function of the flux at that particular location. Zeros in the main diagonal, noticeable as gaps in the figure, represent the void cells added to the corners of the geometry. The gaps introduced by voids can similarly be seen in the diagonals of the diffusion matrix.

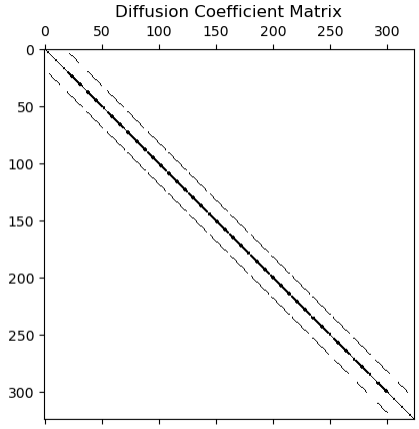

Figure 2: Diffusion Coefficient Matrix

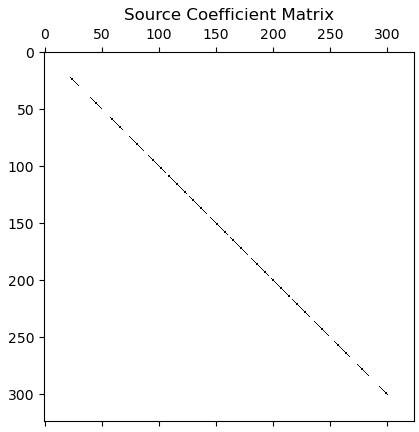

Figure 3: Source Coefficient Matrix

Acknowledging the expected k_{eff} value of 1.025105, the analysis of the simulation results reveals a consistent overestimation of reactivity, as indicated by the calculated k_{eff} values across different cell scalings given in Table 1. The deviation from the expected value decreases with the refinement of the mesh, which suggests that the accuracy of the reactor model improves with a more granular approach to the geometry discretization. Particularly, the finest mesh, h = 0.25 R_{sl}, results in a percent error of approximately 13.95%, a significant improvement over the coarser meshes. This underlines the importance of mesh resolution in the numerical simulation of nuclear reactors, where finer meshes capture the physical phenomena with greater fidelity. This is especially true for reactor schematics with lots of different materials and complex boundary geometry.

Table 1: Simulation Results

Cell Scaling	Cell Side Length [cm]	k_{eff}	% Error	# Iterations
1	23.1226	1.370122	33.65	445
2	11.5613	1.364898	33.14	383
4	5.78065	1.168066	13.95	450

The results from group 2's flux and leakage distributions are particularly noteworthy. Plots given are for h = 0.25 R_{sl}, though there was little difference visuallyfor the other two scaling schemes. The group 2 flux, shown in Figure 5, showcases a distribution with two pronounced peaks along the reactor's periphery, which may be indicative of the second harmonic in neutron flux distribution. This mode, often characterized by its dipole nature, suggests a non-uniform power distribution that could arise from several factors, such as anisotropic neutron leakage, asymmetries in the reactor geometry or material properties, or even from initial conditions that favor this mode. However, the absence of a similar pattern in group 1's results, which displays an unexpected zero flux and leakage as shown in Figure 4,

points to a potential discrepancy in the simulation or the boundary conditions applied. The localized spike in group 2 leakage shown in Figure 5 further accentuates this anomaly, deviating from the anticipated symmetrical leakage pattern typically observed in a homogeneously reacting system. This could be indicative of an issue with the boundary conditions applied in the simulation, particularly around the corners where the boundary conditions may not be properly represented. Alternatively, this could also be a manifestation of an overly simplistic interpretation of the vacuum boundary conditions or a computational artifact introduced by the numerical scheme employed.

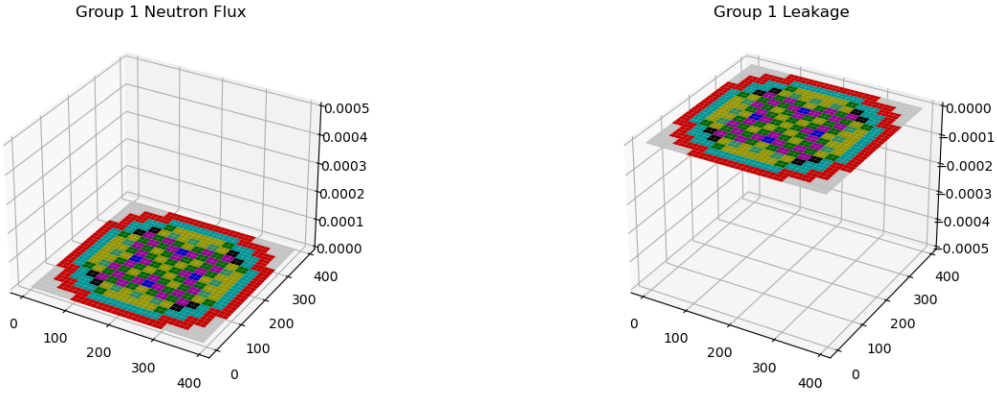

Figure 4: Group 1 Flux and Leakage

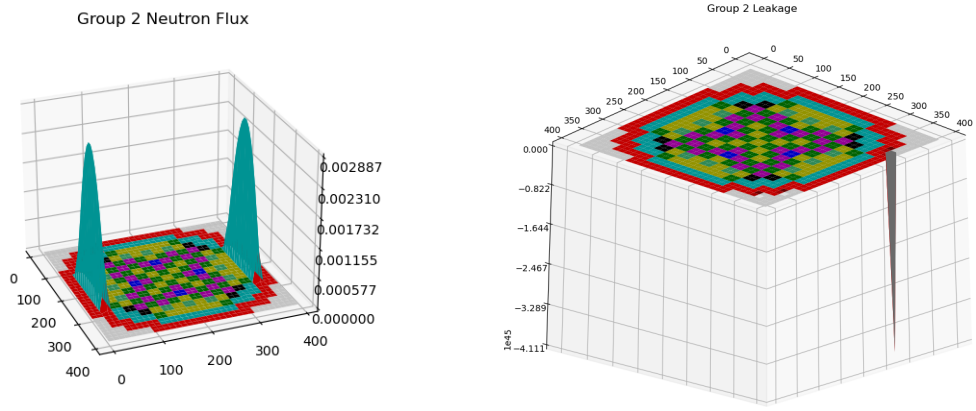

Figure 5: Group 2 Flux and Leakage

In scrutinizing the simulation outcomes, a stark contrast is observed between the neutron flux and leakage distributions for group 1 and group 2. For group 1, both the flux and leakage are unexpectedly registering as zero across the entire domain, as depicted in Figure 4. This uniform absence of flux and leakage contradicts expected physical behavior and implies potential errors in either the boundary conditions, the simulation inputs, or the numerical methods used to solve the diffusion equation.

Turning attention to group 2, the flux distribution presents a strikingly different picture, with two distinct peaks at opposing edges of the reactor, as presented in Figure 5. This pattern is reminiscent of a dipole, which in the context of neutron flux, refers to the second fundamental mode of neutron distribution. Unlike the first mode, which is generally uniform and characterizes a fundamental reactor state, the dipole mode signifies a distribution with two regions of high neutron density separated by a node, or a region of lower neutron density. This kind of distribution could suggest asymmetric conditions within the reactor, such as non-uniformity in reactor composition, irregularities in the geometry, or localized discrepancies in neutron leakage, which could be due to physical asymmetries or an initial state that predisposes the system to this mode. The group 2 leakage exhibits an unexpected localized spike, as highlighted in Figure 6, breaking from the symmetry typical in a balanced reactor system. This anomaly may point to a flaw in how vacuum boundary conditions are applied, particularly at the geometric boundaries where the treatment of corner cells may be inaccurate. Such a localized increase in leakage could also stem from an oversimplified application of boundary conditions or a numerical artifact inherent to the chosen computational approach. These findings call for a methodical verification of the simulation framework. The null results for group 1 flux and leakage need thorough investigation to rectify any computational inaccuracies, while the unexpected dipole pattern in group 2 flux warrants a deeper analysis of the physical modeling and input parameters.

The aforementioned discrepancies in the simulation results necessitates further examination. The absence of group 1 flux and leakage suggests possible computational or boundary condition inaccuracies that must be explored. The observed dipole pattern in group 2 flux, alongside the localized leakage spike, raises questions about the physical representation within the model, such as asymmetries or anisotropic effects not captured by the current framework. The significant deviation of the k_{eff} values from the expected benchmarks, underscores the need for additional validation and refinement of the simulation methodology. Future work should focus on enhancing the mesh resolution, rigorously verifying the input parameters, and reviewing the application of boundary conditions and the inclusion of void cells.

Appendix

See attached PDF file for Python code.